REGIONAL BODY-WAVE DISCRIMINATION RESEARCH

William R. Walter, Arthur Rodgers, Kevin Mayeda and Steve Taylor*
Lawrence Livermore National Laboratory and *Los Alamos National Laboratory

Sponsored by U.S. Department of Energy
Office of Nonproliferation Research and Engineering
Office of Defense Nuclear Nonproliferation
National Nuclear Security Administration

Contract No. W-7405-ENG-48

ABSTRACT

Monitoring the world for potential nuclear explosions requires identifying them by their expected seismic signatures and discriminating them from earthquakes and other sources of seismic waves. Large events (approximately m_b > 4.0) can often be successfully identified by the M_S:m_b discriminant. In order to monitor small events (approximately m_b < 4.0) short-period regional waveform data recorded within 2000 km will be needed because of poor signal-to-noise at large distances and/or long-periods. Many studies have shown that short-period (0.5-10 Hz) regional body wave phases (e.g. Pn, Pg, Sn, Lg and coda) have excellent discrimination power down to very small magnitudes when used at various nuclear tests sites. In order to broaden the application of these regional body wave techniques, we are developing size-, distance- and location-based corrections to apply to the regional data to allow wider data comparison and better discrimination performance.

Building on prior work (e.g. Taylor et al. 1999, Rodgers and Walter, 2000), we are developing a revised Magnitude and Distance Amplitude Correction (MDAC) procedure. The procedure makes use of the very stable moment magnitude determinations from regional coda envelopes (see Mayeda et al, this Symposium) to provide an independent size estimate. Using a Brune (1970) style omega-squared source spectral model, we parameterize the source in terms of apparent stress and its scaling with moment. For the distance corrections we parameterize in terms of geometrical spreading, and frequency-dependent attenuation. In addition there are constants associated with velocities, densities and a phase- and frequency-dependent site effect. Using this relatively simple model we can remove much of the magnitude and distance trends from the regional data. We use a grid-search technique to explore the model space with more emphasis on removing the magnitude and distance trends than in fitting the observable spectra perfectly. Two-dimensional path effects are currently corrected by kriging the MDAC residuals but they could also be addressed through location-dependent attenuation models if available.

Using earthquake and explosion data from the Nevada Test Site and India we show that the revised MDAC correction and kriging of the residuals can significantly improve phase and spectral ratio discrimination performance. In addition by correcting the regional amplitudes we allow maximum flexibility in exploring and creating new combinations of regional phases which may have even better discrimination potential. Finally the corrected regional amplitudes provide critical information on the detection of regional phases, which is another important factor in the overall estimation of discrimination capability.

Key Words: seismic, regional, discrimination, explosion identification, short-period body waves

OBJECTIVES

Monitoring the world for potential nuclear explosions such as for the Comprehensive Nuclear-Test-Ban Treaty (CTBT) requires characterizing seismic events and discriminating between earthquakes, mining activities and banned nuclear tests. We are developing, testing and refining size, distance and location based regional seismic amplitude corrections to facilitate the comparison of all events that are recorded at a particular seismic station. These corrections, calibrated for each station, reduce amplitude measurement scatter and improve discrimination performance. We test the methods on well known (ground truth) datasets in the U.S. and then apply them to the uncalibrated stations in Eurasia, Africa and other regions of interest to improve underground nuclear test monitoring capability.

RESEARCH ACCOMPLISHED

As part of the overall Department of Energy Ground-based Nuclear Explosion Monitoring (GNEM) program, we continue to pursue a comprehensive research effort to improve our capabilities to seismically characterize and discriminate underground nuclear tests from other natural and man-made sources of seismicity. To reduce the monitoring magnitude threshold we make use of regional body wave data and calibrate each seismic station. Our goals are to reduce the variance and improve the separation between earthquakes and explosion populations by accounting for the effects of propagation and differential source size. Building on prior work (e.g. Taylor et al., 2000; Rodgers and Walter, 2000) we are developing a revised Magnitude and Distance Amplitude Correction (MDAC) procedure. Here we briefly review the problem and previous work and then discuss the revised MDAC technique.

Context and NTS Examples

In recent years many studies at nuclear test sites have demonstrated that particular ratios of the amplitudes of regional phases (Pn, Pg, Sn, Lg and coda) have the power to separate explosions from earthquakes, particularly at high frequencies (e.g. Walter et al. 1995, Hartse et al., 1997). For example, Figure 1 shows the comparison of a Nevada Test Site (NTS) nuclear explosion at Rainier Mesa with a nearby earthquake. These events have epicenters within a few kilometers of each other and are nearly the same size or magnitude. The waveforms on the right-hand side of the figure show the differences in the regional phase amplitudes, particularly Lg at 6-8 Hz, as seen at the regional station MNV (a broadband element of the International Monitoring System (IMS) primary array at NVAR). The large contrast in regional phase amplitudes between the two types of events is due to differences in the depth, focal mechanism, source spectra and the medium properties. The exact partitioning of each of these differences in the overall contrast in regional phase amplitudes remains an area of vigorous research. It is clear, however, that if we can account for propagation and source size effects, these physical differences provide a clear basis for effective discrimination techniques.

One such discriminant is the ratio of 6-8 Hz Pn amplitudes to 6-8 Hz Lg amplitudes. In Figure 2 we show the effectiveness of this discriminant for a set of NTS earthquakes and explosions described in detail in Walter et al., 1995 (see Figure 6a in that paper). The relatively large Pn phases and weak Lg amplitudes from the explosions lead to large 6-8 Hz Pn/Lg values for these events relative to the earthquakes. For normal depth earthquakes there is almost no overlap with the explosions. Because there is a good physical basis for earthquake and explosion discrimination we expect this discriminant to be effective for future events on or near NTS. The largest events to occur at NTS since the original study of Walter et al. (1995) was completed was the Frenchman Flat sequence that occurred in January 1999 (K. Smith, pers. Comm.). There were four events larger than magnitude 3.5 with the largest event having an Mw of 4.8 (Walter and Mayeda, 1999). We have processed them using the same techniques as in Walter et al., (1995) and they are plotted for comparison with the original events in Figure 2. Note that they plot within the normal earthquake population and continue to discriminate from the explosions. This gives us confidence we can identify any future events at NTS using these calibrated measurements

Because the events in Figure 2 are all within 50 km or so of each other, and situated within a similar crustal structure and tectonic setting, we expect relatively little difference in the path effects between these events and the stations MNV and KNB. Also because this discriminant measure uses phases at the same frequency band, we expect little or no dependence on source size or magnitude. This allows us to compare all these events together without source or path corrections. If we chose to compare two regional phase amplitudes at different frequencies, such as 1-2Hz Lg to 6-8 Hz Lg, then there is a strong magnitude effect because of the different spectral corner frequencies for small and large events (e.g. Walter and Priestley, 1991, Taylor and Denny, 1991). We show this example in Figure 3 based on the Walter et al., (1995) NTS data (see Figure 8a in the original paper). Note that a magnitude 3 explosion

and a magnitude 5 earthquake have very similar values for the Lg 1-2/6-8 Hz ratio, leading to an ineffective discriminant unless the magnitude difference is accounted for.

We can model the magnitude dependence of regional phase spectral ratios by accounting for the corner frequency differences using a spectral model such as Brune (1970) for earthquakes and Denny and Goodman (1990) for explosions. For explosions we additionally note that events in unsaturated, high gas porosity material above the water table have steeper (f^{-3}) spectral fall off at frequencies above the corner frequency than earthquakes or explosions in saturated material (f^{-2}) do. This is reflected in the model as shown at the top right hand side of Figure 3. The material property effect also can affect the corner frequency scaling as illustrated. A second effect, the scattering and conversion of Rg to S waves (e.g. Myers et al., 1999) introduces an additional frequency dependence to explosion S-wave spectra as shown at the bottom right of Figure 3. Taking all these effects together we can model the behavior of the spectral ratio discriminant reasonably well as shown by the model curves in Figure 3.

Now we are ready to address the question of analyzing new events, which may be located far from any reference explosion data and of a quite different magnitude than any previous explosions. In this case we need to correct for the different paths traveled by the event and the different source spectral scaling introduced by the magnitude differences. Previously we have done this both by correcting the amplitudes (e.g. Taylor et al., 2000) and by correcting the discriminant ratios (Rodgers and Walter, 2000). We have demonstrated that the two techniques give identical answers when carefully done. While the ratios have some advantages in the stability of the search for optimal corrections (since ratios cancel a number of terms), the amplitude correction is more general and has utility for estimating the detectability of regional phases as well. Therefore we will focus on corrections to amplitudes. Here we will briefly review the Magnitude and Distance Amplitude Corrections (MDAC) procedure (Taylor et al., 2000) and describe some revisions that we are starting to implement.

Revised MDAC

The basic MDAC procedure involves estimating and removing a simple theoretical earthquake spectrum from the data to remove any magnitude and distance trends in the regional phase amplitudes and any discriminants formed from those amplitudes (Taylor et al., 2000). The observed regional phase spectra are modeled as:

$$P(f,R) = I(f)\, S(f)\, G(f,R)\, A(f,R) \qquad (1)$$

where f is frequency and R is distance and:

I(f) is the instrument response,
S(f) is the source spectrum from the Brune (1970) model,
G(f,R) is the earth response, modeled as proportional to Site(f) R^{η},
A(f,R) is the apparent attenuation, modeled as $e^{(-\pi f R/Q(f)c)}$,

c is the velocity of the phase and Q(f) is the frequency dependent quality factor.

In addition the source spectrum depends upon the seismic moment and stress drop and can have additional complications due to non-constant stress drop scaling and differential P/S corner frequency effects that we will discuss later. We require the different phases for the same event recorded at the same station to have the same moment values and any other source parameters, such as stress drop or corner frequencies to be related to each other. This effectively imposes some of the ratio constraints discussed in Rodgers and Walter (2000) on the amplitudes and improves discrimination performance. While such models of observed spectra are certainly oversimplified, they have proven track records of providing good first-order fits to real earthquakes. In addition they also provide simple theoretical models to use in aseismic areas.

To estimate the source spectrum we first need an estimate of the seismic moment. In the revised MDAC procedure we take advantage of the very stable moment magnitude determinations from regional coda envelopes (see Mayeda et al., this volume). The coda-based technique provides an accurate and independent estimate of moment from as few as one station. Using a direct measure of moment also eliminates the need to scale from other magnitudes such as m_b to moment eliminating two fitting parameters from the original formulation (Taylor et al, 2000). The combination of using the more stable coda measure and eliminating two free parameters should reduce scatter in the resulting correction.

We show an example of the revised MDAC fits using the coda-based moment magnitudes (M_w) in Figure 4 for three NTS earthquake Lg spectra recorded at KNB. The earthquakes are the June 1992 Little Skull Mountain mainshock and two aftershocks and cover two orders of magnitude in size. The M_w values were calculated in a previous study by Mayeda and Walter (1996) using the regional coda technique at two stations, MNV and KNB. The left-hand side of Figure 4 shows that using a constant stress drop model does not fit all the data simultaneously. In this case we used a Brune stress drop of 30 bars, which provides a good fit to the mainshock but not the smaller aftershocks. The aftershocks require lower stress drops to match the observed spectra, consistent with the observations of Mayeda and Walter (1996) using the coda-based source spectra determinations. A problem with non-constant stress drop scaling is that the Brune (1970) model is specifically set up as constant stress drop model. Taylor et al. (2000) have implemented a non-constant scaling, which we used in Figure 4, but at a cost of the stress drop becoming a non-physical parameter. This means we can no longer interpret a stress drop in terms of bars in the non-constant scaling case. This is somewhat unsatisfactory both theoretically and practically when we want to use the MDAC formulation in regions without data where parameters like stress drop may be determined from models.

In the second revision to MDAC we reformulate the Brune (1970) source spectrum in more general terms. The Brune (1970) spectral shape is given by:

$$S(f) = S_o / (1 + (f/f_c)^2) \qquad (2)$$

where S_o is the zero frequency spectral level and f_c is the corner frequency. We parameterize S_o using the seismic moment and the well known relationship between them (e.g. Aki and Richards, 1980):

$$S_o = R_{\theta\varphi} M_o / (4\pi\rho_r\rho_s c_s^5 c_r)^{1/2} \qquad (3)$$

where $R_{\theta\varphi}$ is the radiation pattern coefficient appropriate to the given wave type, ρ is the density, c is the velocity of the given wave type and the subscripts r and s refer to the receiver and source region respectively. Note we have removed the geometrical spreading term to a separate G(f,R) function in equation (1). To parameterize the corner frequency, we reformulate the stress drop in terms of a more general stress parameter, the apparent stress (e.g. Wyss, 1970):

$$\sigma_a = \mu E / M_o \qquad (4)$$

where E is the seismically radiated energy and μ is the rigidity. The seismically radiated energy in any particular wave type with velocity c and a spectrum given by equation (2) can be determined by integrating to find (Walter and Brune, 1993):

$$E_c = \pi\rho_r c_r S_o 2 f_c^3 = R_{\theta\varphi}^2 M_o^2 f_c^3 / (16\pi\rho_s c_s^5) \qquad (5)$$

where we used equation (3) to put it in terms of seismic moment. Note again we have removed the geometrical spreading term since it appears separately in G(f,R). Equation (5) can now be used with equation (4) to determine the corner frequency scaling for a particular phase.

To keep the source parameters related we want to use a single apparent stress parameter for each event and therefore we sum the energy from all the regional phases (e.g. Pn, Pg, Sn and Lg) to find the total radiated body-wave energy to put into equation (4). For simplicity we group the P-waves and S-waves together and use an additional parameter to link the P- and S wave corner frequencies:

$$f_{c\alpha} = x f_{c\beta} \qquad (6)$$

where subscripts α and β denote P- and S-wave corner frequencies and x is the scale factor. For the Brune (1970) model x is the ratio of the wave velocities, but other studies have shown that the corner frequencies are more equal (x=1), by including this parameter we allow maximum flexibility. We treat the energy radiated as the simple sum of P and S wave energy and use equations (4), (5) and (6) to solve for the S–wave corner frequency:

$$f_{c\beta} = (k\sigma_a / M_o)^{1/3} \qquad \text{where } k = 16\pi\rho_s / (\mu(x^3 R_{\theta\varphi\alpha}^2/\alpha_s^5 + R_{\theta\varphi\beta}^2/\beta_s^5)) \qquad (7)$$

so that for constant apparent stress the corner frequency scales as $M_o^{-1/3}$ as in the Brune (1970) model. This formulation using equation (7) allows us to put in physical non-constant apparent stress scaling by changing the apparent stress with moment. Now for example we can use the quarter root scaling observed by Mayeda and Walter

(1996) for Western U.S. earthquakes to improve the spectral fits. For example the earthquakes in Figure 4 have apparent stress values ranging from 196 bars for the mainshock to 20 for the smaller aftershock and we have agreement between the coda determined values and those in the revised MDAC. Equations 1-7 with the independent coda determined seismic moments constitute the revised MDAC procedure.

So far we have used the revised MDAC to correct for trends in Magnitude and Distance, but there are also variations due to the spatial variability of events, for example events occurring in very different tectonic regions. We account for much of this effect empirically by kriging the MDAC residuals using the Bayesian technique developed by Schultz et al, (1998) and shown to be very effective for discriminants (e.g. Rodgers et al., 1999). However in cases where empirical data is lacking, we want to allow the apparent attenuation function to vary spatially as well. This way we can make use of a prior information such as that produced by attenuation tomography (e.g. Phillips et al., 2000), or other geophysical studies. Allowing the attenuation to become a function of location is the last part of the revised MDAC procedure. Finally, by removing the magnitude and distance trends from the data, we allow the combination of individual measures, to form a multivariate discriminants that can be significantly more effective than the best individual measure (e.g. Taylor, 1996).

CONCLUSIONS AND RECOMMENDATIONS

Regional discrimination algorithms require calibration at each seismic station to be used for nuclear explosion monitoring. We have developed a revised Magnitude and Distance Amplitude Correction procedure to remove source size and path effects from regional body-wave phases. This allows the comparison of any new regional events recorded at a calibrated station with all available reference data and models. This also facilities the combination of individual measures to form multivariate discriminants that can have significantly better performance. We will show that this revised MDAC improves regional earthquake and explosion discrimination on a test set of events in the western U.S. and other regions of the world. Calibrating seismic stations for monitoring the CTBT is a challenging task that will require processing large amounts of data, and collaboration with government, academic and industry researchers and incorporation of the extensive R&D results both within and outside of DOE.

ACKNOWLEDGEMENTS

This work performed under the auspices of the U.S. Department of Energy by the Lawrence Livermore National Laboratory under contract W-7405-ENG-48. UCRL-JC-138998.

REFERENCES

Aki, K. and P. G. Richards, (1980). *Quantitative Seismology*, W. H. Freeman, New York.

Brune, J., (1970). Tectonic stress and the spectra from seismic shear waves earthquakes, *J. Geophys. Res*., **75**, 4997-5009.

Denny, M. D. and D. M. Goodman, (1990). A case study of the seismic source functions SALMON and STERLING reevaluated, *J. Geophys. Res. 95*, 19,705-19,723.

Hartse, H., S. R. Taylor, W. S. Phillips, and G. E. Randall, (1997). A preliminary study of regional seismic discrimination in Central Asia with an emphasis on Western China*, Bull. Seism. Soc. Am.* **87**, 551-568.

Mayeda, K. M. and W. R. Walter, (1996). Moment, energy, stress drop and source spectra of Western U.S. earthquakes from regional coda envelopes, *J. Geophys. Res*., **10***1*, 11,195-11,208.

Myers, S. C., W. R. Walter, K. Mayeda and L. Glenn, (1999). Observations in support of Rg scattering as a source for explosion S waves: regional and local recordings of the 1997 Kazakhstan depth of burial experiment, *Bull. Seism. Soc. Am. 89*, 544-549.

Phillips, W. S., H. E. Hartse, S. R. Taylor, A. A. Velasco and G. E. Randall, (2000). Regional phase amplitude ratio tomography for seismic verification, Los Alamos National laboratory, LAUR-99-1904, submitted to *Pure. App. Geophys*.

Rodgers, A. J., W. R. Walter, C. Schultz and S. Myers, (1999). A comparison of methodologies for representing path effects on regional P/S discriminants, *Bull. Seism. Soc. Am. 89*, 394-408.

Rodgers, A. J. and W. R. Walter, (2000). Seismic Discrimination of the May 11, 1998 Indian Nuclear Test with Short-Period Regional Data From Station NIL (Nilore, Pakistan), submitted to PAGEOPH.

Schultz, C., S. Myers, J. Hipp, and C. Young, (1998). Nonstationary Bayesian kriging: application of spatial corrections to improve seismic detection, location and identification, *Bull. Seism. Soc. Am., 88*, 1275-1288.

Taylor, S. and M. Denny, (1991). An analysis of spectral differences between NTS and Shagan River nuclear explosions, *J. Geophys. Res.*, **96**, 6237-6245.

Taylor, S., (1996). Analysis of high-frequency Pg/Lg ratios from NTS explosions and Western U.S. earthquakes, *Bull. Seism. Soc. Am., 86*, 1042-1053.

Taylor, S., A. Velasco, H. Hartse, W. S. Philips, W. R. Walter, and A. Rodgers, (2000). Amplitude corrections for regional discrimination, submitted to *Pure. App. Geophys.,* 2000

Walter, W., and K. Priestley, (1991). High-frequency P wave spectra from explosions and earthquakes, in *Explosion Source Phenomenology*, ed. S. Taylor, H. Patton and P. Richards, American Geophysical Union Monograph.

Walter, W. R. and J. N. Brune, (1993). Spectra of seismic radiation from a tensile crack, *J. Geophys. Res., 98*, 4449-4459.

Walter, W. R., K. Mayeda, and H. J. Patton, (1995). Phase and spectral ratio discrimination between NTS earthquakes and explosions Part 1: Empirical observations, *Bull. Seism. Soc. Am.,* **85**., 1050-1067.

Walter, W. R. and K. Mayeda, (1999). LLNL Nevada test site seismic event report, Bulletin 99-02, Lawrence Livermore National Laboratory UCRL-MI-133002-99-02.

Wyss, M., (1970). Stress estimates of South American shallow and deep earthquakes, *J. Geophys. Res., 75*, 1529-1544.

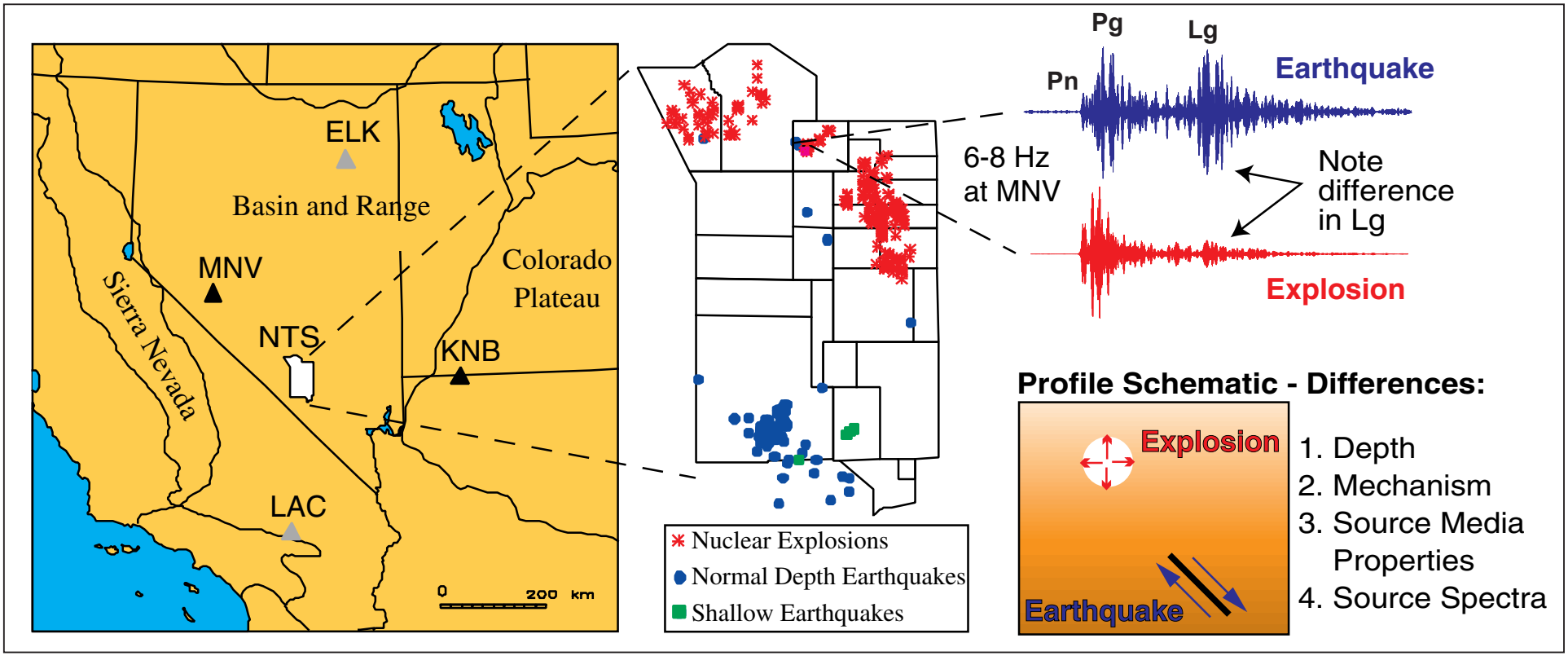

Fig. 1. An example of regional body-wave discrimination at the Nevada Test Site (NTS). The left-hand map shows the location of NTS in relation to the regional seismic stations MNV (Mina, Nevada) and KNB (Kanab, Utah), part of the four station LLNL NTS network. The expansion of NTS (center) shows the location of about 50 earthquakes and 120 explosions used in an earlier discrimination study by Walter et al. (1995). The top left-hand seismograms compare an earthquake and an explosion of similar size and with very closely located epicenters. Note that at this high-frequency passband of 6-8 Hz, there is a significant difference in the Lg amplitude compared with the Pn or Pg amplitudes between the two events. These relative phase amplitude differences are caused by differences in depth, mechanism, source medium properties and source spectra as outlined on the lower left. These physical differences lead to the ability to discriminate earthquakes from explosions for nearly co-located, equal size events. To compare events of different sizes and locations, we must account for source size and path effects, which is the subject of this paper.

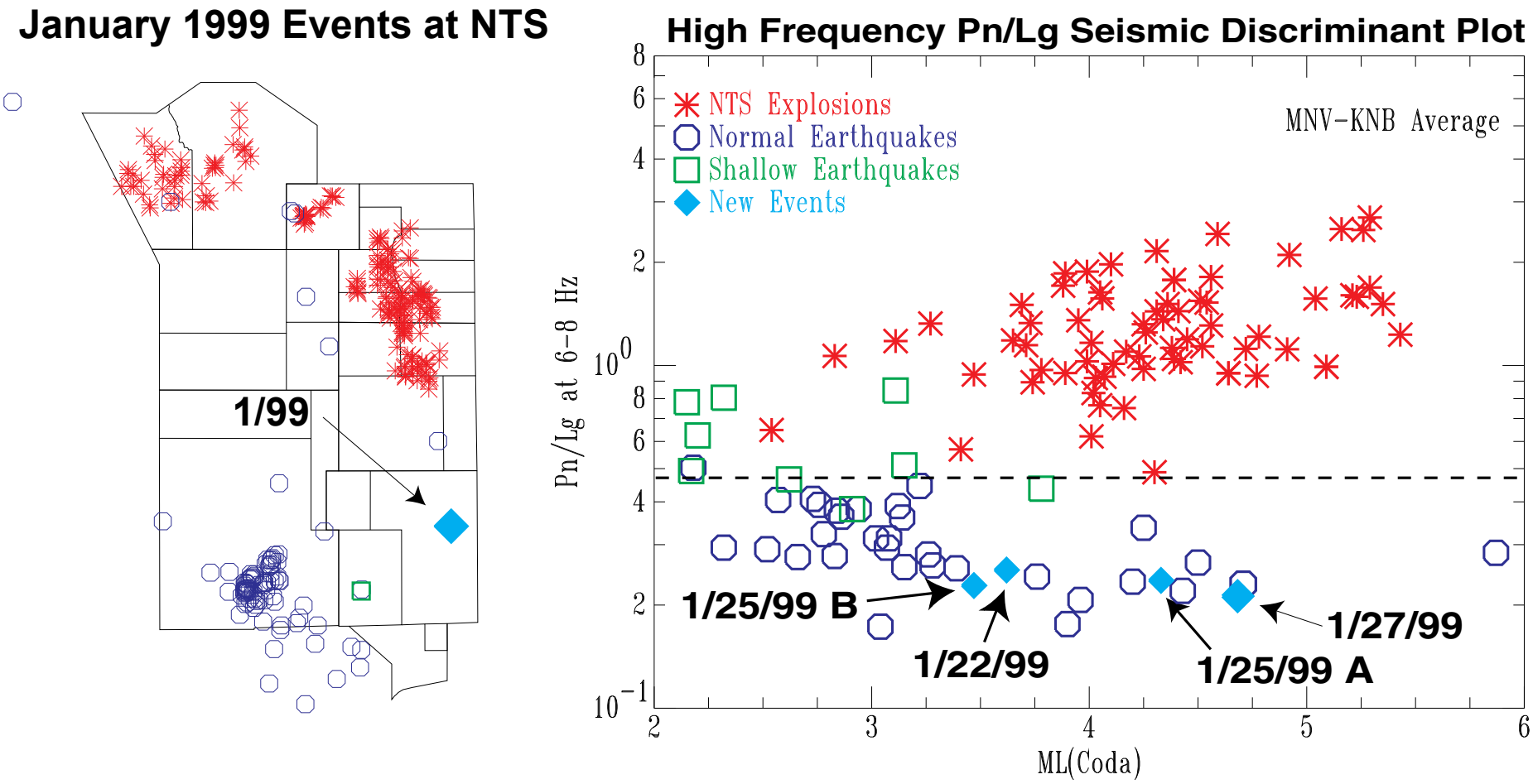

Fig. 2. An example of discrimination results for recent NTS earthquakes compared with historical data from an earlier study. The left-hand map shows the location of the events, the right-hand plot shows the 6-8 Hz Pn/Lg discriminant averaged over values from MNV and KNB (both must exist and pass signal-to-noise tests). The base plot is after Figure 6 of Walter et al. (1995). Note the almost complete separation of normal depth earthquakes and explosions. In January 1999 a vigorous earthquake sequence occurred in the Frenchman flat region of NTS, with four events over moment magnitude 3.5, the largest Mw=4.8 (Walter and Mayeda, 1999). This is the largest earthquake to occur at NTS since the 1992 Little Skull Mountain events. Processing these new events in the same manner as in the earlier study we find they plot in the earthquake population and discriminate well from the explosions. This gives us confidence in our ability to identify new earthquakes at NTS using our calibrated discriminants.

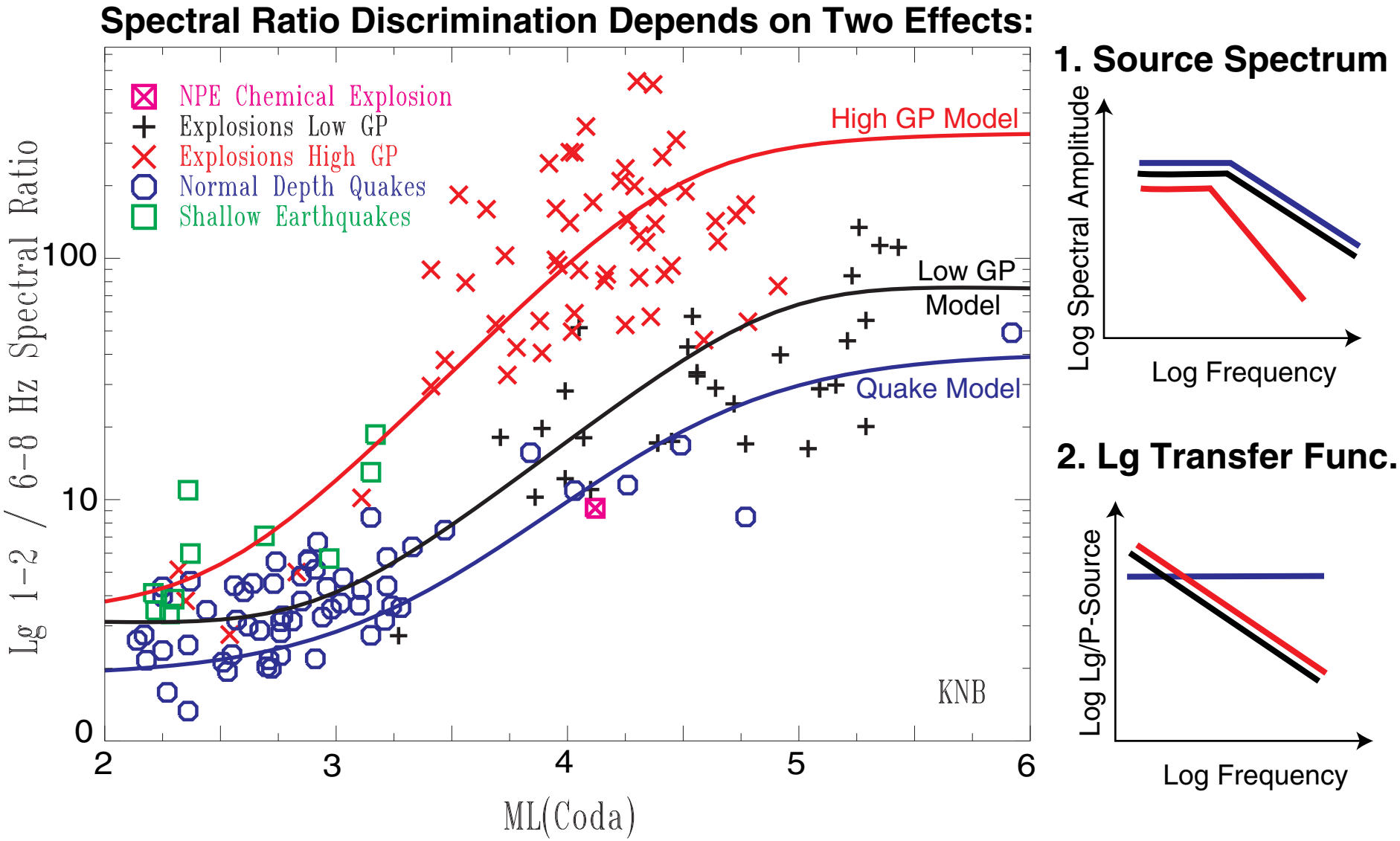

Fig. 3. An example of the magnitude dependence of ratios using amplitudes in different frequency bands. The left-hand plot shows the Lg 1-2/6-8 Hz spectral ratio after Figure 8a of Walter et al., (1995). We model the spectral ratio values using two effects. First we use source spectral models for the earthquakes and explosions. The earthquakes and low gas porosity (GP) explosions have high-frequency fall off as f^{-2} while the high gas porosity events have steeper f^{-3} fall off at high frequencies. As the two frequency measures at 1-2 Hz and 6-8 Hz move from both being on the flat part of the spectrum for small magnitude events to both being on the falling-off part of the spectrum for large magnitude events, they trace out a characteristic sigmoid shape as shown in the model curves. This is the magnitude dependence we seek to remove with the MDAC procedure. In addition the explosion models are offset from the earthquakes due to the second effect, the scattering and conversion of Rg and P energy to Lg energy. This is a frequency dependent transfer function (e.g. Myers et al., 1999) and depends on the shallow depth of the explosions and the velocity structure and other near-source effects.

An example of MDAC fits to Lg spectra from the 1992 Little Skull Mountain sequence at the Nevada Test Site: Mainshock and two aftershocks.

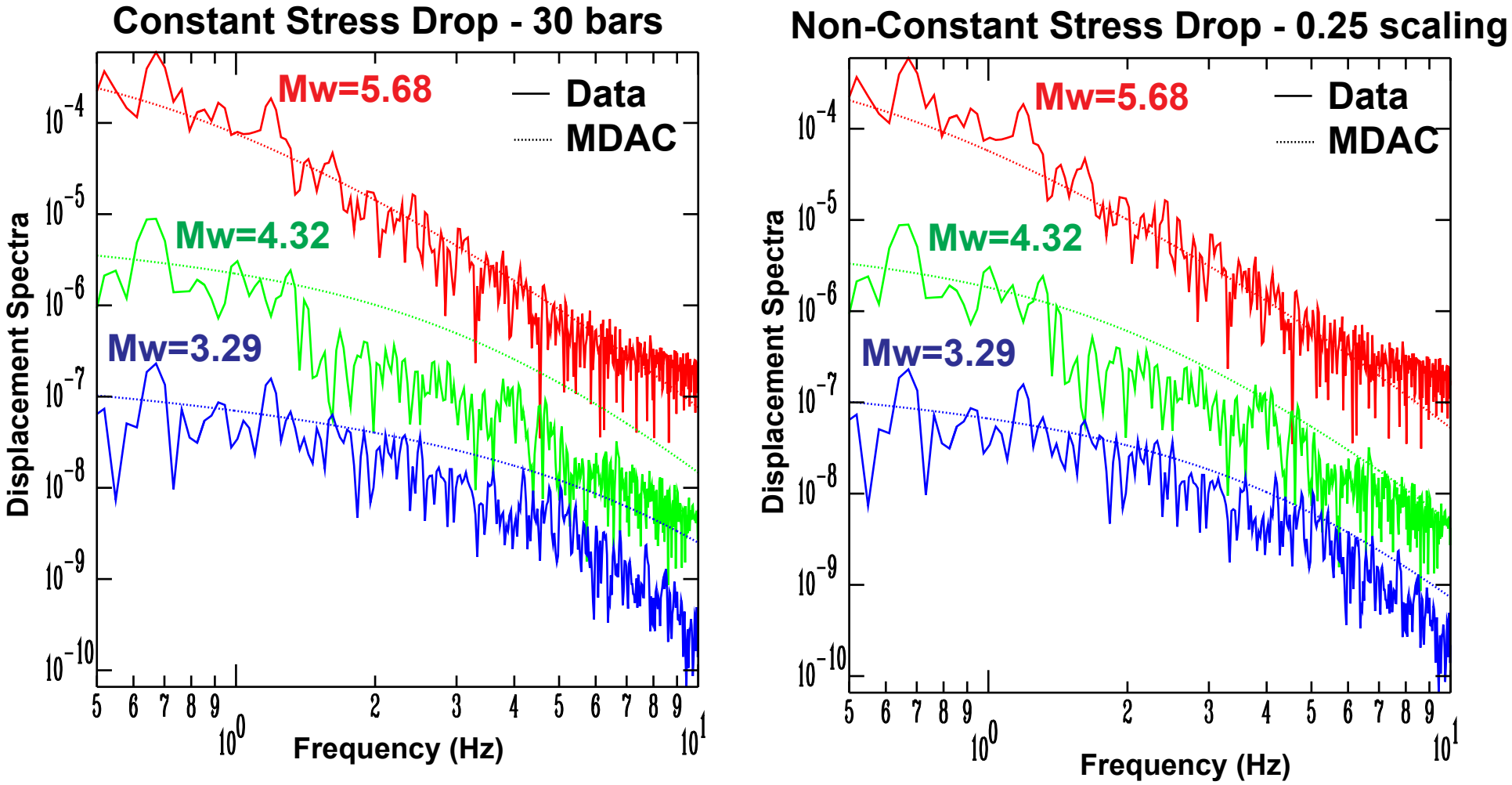

Fig. 4. Example of MDAC Lg spectral fits to three NTS earthquakes recorded at station KNB. The largest event is the June 29, 1992, Little Skull Mountain mainshock, and the smaller events are two aftershocks. The moment magnitudes come from a study by Mayeda and Walter (1996) that used regional coda envelopes and a set of corrections to determine source spectra, moments and stress drops of a number of Western U.S. earthquakes. We tried fitting these events with both constant stress drop models (left) and quarter root stress drop scaling (right). Note the quarter root scaling produces better fits and is consistent with the independent coda results of Mayeda and Walter (1996).